

Alma Mater Studiorum Università di Bologna
Archivio istituzionale della ricerca

Modulating the water oxidation catalytic activity of iridium complexes by functionalizing the Cp*-ancillary ligand: hints on the nature of the active species

This is the final peer-reviewed author's accepted manuscript (postprint) of the following publication:

Published Version:

Gatto G., De Palo A., Carrasco A.C., Pizarro A.M., Zacchini S., Pampaloni G., et al. (2021). Modulating the water oxidation catalytic activity of iridium complexes by functionalizing the Cp*-ancillary ligand: hints on the nature of the active species. CATALYSIS SCIENCE & TECHNOLOGY, 11(8), 2885-2895 [10.1039/d0cy02306j].

Availability:

This version is available at: <https://hdl.handle.net/11585/848325> since: 2022-01-27

Published:

DOI: <http://doi.org/10.1039/d0cy02306j>

Terms of use:

Some rights reserved. The terms and conditions for the reuse of this version of the manuscript are specified in the publishing policy. For all terms of use and more information see the publisher's website.

This item was downloaded from IRIS Università di Bologna (<https://cris.unibo.it/>).
When citing, please refer to the published version.

(Article begins on next page)

This is the final peer-reviewed accepted manuscript of:

G. Gatto, A. De Palo, F. Marchetti, A. C. Carrasco, G. Pampaloni, A. M. Pizarro, S. Zacchini, A. Macchioni, "Modulating the Water oxidation Catalytic activity of Iridium Complexes by Functionalizing the Cp*-Ancillary Ligand: Hints on the Nature of the Active Species", *Catal. Sci. Technol.*, **2021**, 11, 2885-2895.

The final published version is available online at:

<https://doi.org/10.1039/d0cy02306j>

Rights / License: Licenza per Accesso Aperto. Creative Commons Attribuzione - Non commerciale - Non opere derivate 4.0 (CCBYNCND)

The terms and conditions for the reuse of this version of the manuscript are specified in the publishing policy. For all terms of use and more information see the publisher's website.

This item was downloaded from IRIS Università di Bologna (<https://cris.unibo.it/>)

When citing, please refer to the published version.

Modulating the Water oxidation Catalytic activity of Iridium Complexes by Functionalizing the Cp^{*} - Ancillary Ligand: Hints on the Nature of the Active Species

Giordano Gatto,[‡] Alice De Palo,[#] Ana C. Carrasco,[¥] Ana M. Pizarro,[¥] Stefano Zacchini,[§] Guido Pampaloni,[#] Fabio Marchetti,^{,#} and Alceo Macchioni^{*,‡}*

[‡]Department of Chemistry, Biology and Biotechnology and CIRCC, University of Perugia, Via Elce di Sotto 8, 06123 Perugia, Italy. [#]Dipartimento di Chimica e Chimica Industriale University of Pisa, Via G. Moruzzi 13, 56124 Pisa, Italy. [¥]IMDEA Nanociencia, Ciudad Universitaria de Cantoblanco, 28049 Madrid, Spain. [§]Dipartimento di Chimica Industriale “Toso Montanari”, Università di Bologna, Viale Risorgimento 4, 40136 Bologna, Italy.

KEYWORDS (Word Style “BG_Keywords”).

ABSTRACT. The catalytic activity of [^RCp^{*}IrCl(μ-Cl)]₂ (R = H, **1**; R = Me, **2**; R = Et, **3**; R = Pr, **4**; R = CH₂CH₂NH₂, **5**; R = Ph, **6**; R = 4-C₆H₄F, **7**; R = 4-C₆H₄OH, **8**; R = Bn, **9**), dimeric precursors toward NaIO₄ driven water oxidation, has been evaluated at 298 K and pH = 7 (by phosphate buffer). For each dimer, the effect of changing catalyst (1-10 μM) and NaIO₄ (5-40 mM) concentration has been studied. All precursors exhibit a high activity with TOF values ranging from

This item was downloaded from IRIS Università di Bologna (<https://cris.unibo.it/>)

When citing, please refer to the published version.

101 min⁻¹ to 393 min⁻¹ and TON values being always those expected assuming a 100% yield. The catalytic activity was strongly affected by the nature of the R substituent. Highest TOF values were observed when R was electron-donating and small.

1. INTRODUCTION

The development of efficient catalysts for water oxidation (WOCs) remains the main obstacle to the assembly of a working device for the production of fuels from renewable sources.¹⁻⁶ Considerable progress has been achieved, over the last few years, with material-based,⁷⁻⁹ heterogenized,¹⁰⁻¹⁵ and molecular WOCs.¹⁶⁻²¹ Among the latter, organoiridium complexes have been successfully exploited as precursors of WOCs.^{22,23} Most of them can be formulated as [Cp*IrL₁L₂X]ⁿ where L₁ and L₂ might be either two monodentate or one bidentate ligand(s), whereas X is H₂O or a labile ligand easily exchangeable with a water molecule. Despite many studies have been performed to understand how the nature of L₁ and L₂ affect WO performances, to the best of our knowledge, very little (or no) attention has been dedicated to explore the possible effect of functionalizing the Cp* ancillary ligand.²⁴ This is probably due to the difficulty of synthesizing Cp*-substituted precursors and also to the belief that Cp* is easily lost under the strongly oxidative conditions used in WO catalysis. As a matter of fact, many studies, initially carried out by NMR spectroscopy, indicated that the Ir-C bond of the quaternary Cp* ligand is the weak point of [Cp*IrL₁L₂X]ⁿ WOC,²⁵ which can be easily oxidized opening reaction pathways leading to the oxidative transformation of Cp*, causing the degradation of the latter and formation of small organic molecules such as CH₃COOH, HCOOH, CH₂COOH, and CO₂.²⁶⁻²⁸ At the same time, organometallic species having an oxidatively degraded Cp* still bonded at iridium, but with reduced hapticity, have been observed, in some cases.²⁸ Interestingly, the rate of CH₃COOH and HCOOH formation, two important degradation products of Cp*, was found to be substantially

This item was downloaded from IRIS Università di Bologna (<https://cris.unibo.it/>)

When citing, please refer to the published version.

higher than that of O₂ evolution, indicating that the oxidative degradation occurs in the preliminary stage of the catalysis, likely during the induction time, and leads to the formation of the active species that carry on most O₂ evolution process.²⁹ Nevertheless, to the best of our knowledge, no investigation demonstrated that Cp* is completely degraded during such a preliminary stage. On the contrary, the few attempts aimed at quantifying the small organic oxidized molecules indicated that two/three carbon atoms of Cp* are apparently missing and many hypotheses on the nature of active species of WO have been proposed in which a fragment of the Cp* is present.^{30,31} For instance, Batista suggested that a dimeric species bearing a methyl-acetone-acetonate moiety, bonded at each iridium atom, derived from Cp* oxidative degradation, is present in the active species.³²

In order to shed some light on how the functionalization of Cp* affects WO catalyzed by [Cp*IrL₁L₂X]ⁿ catalysts, we decided to synthesize a series of Ir-dimers with R-functionalized Cp*, i.e. [(η⁵-C₅Me₄R)IrCl(μ-Cl)]₂: R = H, **1**; R = Me, **2**; R = Et, **3**; R = Pr, **4**; R = CH₂CH₂NH₂, **5**; R = Ph, **6**; R = 4-C₆H₄F, **7**; R = 4-C₆H₄OH, **8**; R = Bn, **9**; Figure 1) and test them as WO catalytic precursors. WO catalytic experiments were carried out using NaIO₄ as sacrificial oxidant at pH = 7 (by phosphate buffer) and at 298 K. For each dimer seven experiments were carried out, changing catalyst and NaIO₄ concentration, according to a standardized methodology recently applied by us to benchmarking a rather large number of well-known iridium WOCs.³³

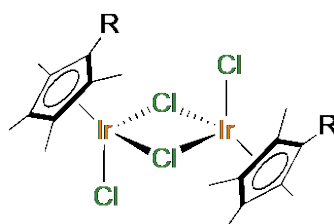


Figure 1: Sketch of the investigated Ir-dimers.

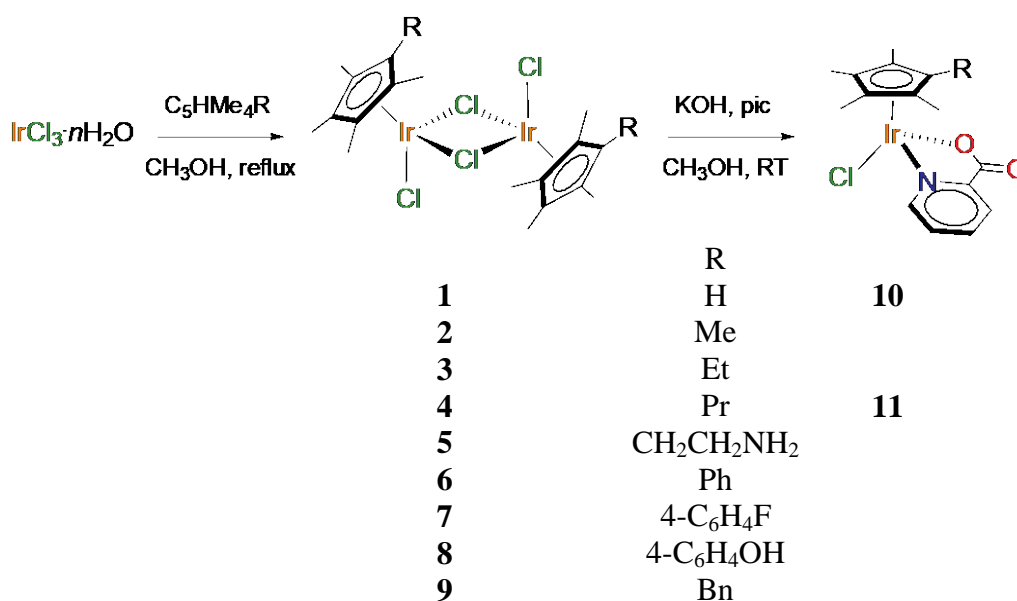
It was found that WO catalytic activity is strongly affected by the nature of R with best performances obtained when electron donating and small R-substituents are used.

2. RESULTS AND DISCUSSION

The di-iridium complexes, including the novel **1**, **3-5**, **7-8**, were obtained in moderate yields using a typical procedure consisting in the reaction of commercial iridium(III) chloride hydrate with the appropriate substituted cyclopentadiene precursor in refluxing methanol (Scheme 1).^{34,35} The cyclopentadiene $C_5HMe_4(4-C_6H_4F)$ is unprecedented, while $C_5HMe_4(4-C_6H_4OH)$ was synthesized by a modified literature method (see Experimental for details).³⁶ Both these pro-ligands were isolated as almost exclusively single isomeric forms.³⁴ In order to prepare **8**, the hydroxyl group of $C_5HMe_4(4-C_6H_4OH)$ was preliminarily protected, then the reaction of $C_5HMe_4(4-C_6H_4OCMe_2OMe)$ with $IrCl_3 \cdot nH_2O$, followed by silica chromatography, directly afforded **8**. The new mononuclear **10** and **11** were obtained from **1** and **4**, respectively, by reaction with picolinic acid (pic) and finally isolated in 40% (**10**) and 76% (**11**) yields. All the iridium complexes, except **8**, are well soluble in chlorinated solvents and exhibit very low solubilities in water and hydrocarbons; instead **8** is almost insoluble in common organic solvents, apart from methanol and DMSO. The new complexes were characterized by elemental analysis, IR and NMR spectroscopy, and their identity was confirmed by mass spectrometry. The 1H and ^{13}C NMR patterns related to the C_5Me_4 unit are consistent with what previously reported for similar dinuclear and mononuclear species.³⁴ The CH moiety belonging to the five-membered ring in **1** gives rise to resonances at 5.30 ppm (1H) and 68.1 ppm (^{13}C). The hydroxyl group in **8** manifests itself with an absorption falling at 3305 cm^{-1} in the IR spectrum (solid state). The ^{19}F NMR resonance due to the fluorine atom undergoes minor shift on going from $C_5HMe_4(4-C_6H_4F)$ (−117.6 ppm) to **7** (−112.7 ppm).

This item was downloaded from IRIS Università di Bologna (<https://cris.unibo.it/>)

When citing, please refer to the published version.



Scheme 1: Synthesis of di- and mono-iridium complexes $[\text{R}^*\text{Cp}^*\text{Ir}(\kappa^2\text{-N,O})\text{Cl}]$ ($\kappa^2\text{-N,O}$ = 2-pyridinecarboxylic acid, ion(-1)). ^a From $\text{C}_5\text{HMe}_4(4\text{-C}_6\text{H}_4\text{OCMe}_2\text{OMe})$.

The molecular structures of **7** and **11** were ascertained by X-ray diffraction studies (Figures 2 and 3).

The molecular structure of **7** is closely related to those previously reported for other chlorido-bridged half-sandwich complexes of the type $[\text{CpIrCl}(\mu\text{-Cl})]_2$, where the Cp ligands were variously functionalized [ref: Tönnemann, J.; Risse, J.; Grote, Z.; Scopelliti, R.; Severin, K. Efficient and Rapid Synthesis of Chlorido-Bridged Half-Sandwich Complexes of Ruthenium, Thodium, and Iridium by Microwave Heating. *Eur. J. Inorg. Chem.* **2013**, 4558-4562; Liu, Z.; Habtemariam, A.; Pizarro, A. M.; Fletcher, S. A.; Kisova, A.; Vrana, O.; Salassa, L.; Bruijninx, C. A.; Clarkson, G. J.; Brabec, V.; Sadler, P. J. Organometallic Half-Sandwich Iridium Anticancer Complexes. *J. Med. Chem.* **2011**, 54, 3011-3026; Chruchill, M. R.; Julis, S. A. Crystal Structure and Molecular Geometry of the Homogeneous Hydrogenation Catalyst $[\eta^5\text{-C}_5\text{Me}_5]\text{IrCl}_2(\mu\text{-H})(\mu\text{-Cl})$ and of Its

This item was downloaded from IRIS Università di Bologna (<https://cris.unibo.it/>)

When citing, please refer to the published version.

Precursor $[\eta^5\text{-C}_5\text{Me}_5\text{IrCl}]_2(\mu\text{-Cl})_2$ - A Direct Comparison of $\text{Ir}(\mu\text{-H})(\mu\text{-Cl})\text{Ir}$ and $\text{Ir}(\mu\text{-Cl})_2\text{Ir}$ Bridging Systems. *Inorg. Chem.* **1977**, *16*, 1488-1494; Park-Gehrke, L. S.; Frudenthal, J.; Kaminsky, W.; DiPasquale, A. G.; Mayer, M. Synthesis and oxidation of $\text{Cp}^*\text{Ir}^{\text{III}}$ compounds: functionalization of a Cp^* methyl group. *Dalton Trans.* **2009**, 1972-1983; Morris, D. M.; McGeagh, M.; De Peña, D.; Merola, J. S. Extending the range of pentasubstituted cyclopentadienyl compounds: The synthesis of a series of tetramethyl(alkyl or aryl)cyclopentadienes ($\text{Cp}^{*\text{R}}$), their iridium complexes and their catalytic activity for asymmetric transfer hydrogenation. *Polyhedron* **2014**, *84*, 120-135; Romanov-Michailidis, F.; Ravetz, B. D.; Paley, D. W.; Rovis, T. Ir(III)-Catalyzed Carbocarbation of Alkynes through Undirected Double C-H Bond Activation of Anisoles. *J. Am. Chem. Soc.* **2018**, *140*, 5370-5374; Brown, L. C.; Ressegué, E.; Merola, J. S. Rapid Access to Derivatized, Dimeric, Ring-Substituted Dichloro(cyclopentadienyl)rhodium(III) and Iridium(III) Complexes. *Organometallics* **2016**, *35*, 4014-4022; Shadap, L.; Joshi, N.; Poluri, K. M.; Kollipara, M. R.; Kaminsky, W. Synthesis and structural characterization of arene d^6 metal complexes of sulfonohydrazones and triazolo ligands: High potency of triazolo derivatives towards DNA binding. *Polyhedron* **2018**, *155*, 302-312; Zhang, P.; Guo, Y.-J.; Chen, J.; Zhao, Y.-R.; Chang, J.; Junge, H.; Beller, M.; Li, Y. Streamlined hydrogen production from biomass. *Nature Catalysis* **2018**, *1*, 332.] The $\text{Ir}(\mu\text{-Cl})_2\text{Ir}$ core is perfectly planar (mean deviation from the least squares plane 0.0079 Å) and the two $^4\text{F-PhCp}^*$ ligands adopt a *pseudo-trans* conformation, as usually found in related complexes.

This item was downloaded from IRIS Università di Bologna (<https://cris.unibo.it/>)

When citing, please refer to the published version.

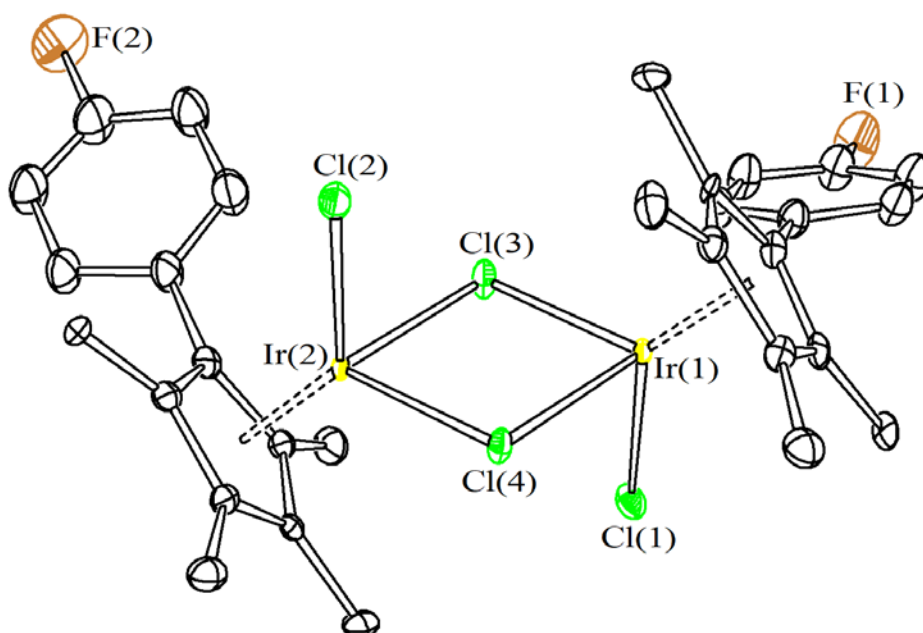


Figure 2. Molecular structure of $[\text{}^{4\text{F-Ph}}\text{Cp}^*\text{IrCl}(\mu\text{-Cl})]_2$, **7**. Displacement ellipsoids are at the 50% probability level. H-atoms have been omitted for clarity. Selected bond lengths (Å) and angles (°): Ir(1)–Cl(1) 2.382(3), Ir(1)–Cl(3) 2.450(3), Ir(1)–Cl(4) 2.457(3), Ir(1)– $^{4\text{F-Ph}}\text{Cp}^*$ 2.115(14)– 2.157(13), Ir(2)–Cl(2) 2.386(3), Ir(2)–Cl(3) 2.442(3), Ir(2)–Cl(4) 2.454(3), Ir(2)– $^{4\text{F-Ph}}\text{Cp}^*$ 2.115(14)– 2.161(13), Cl(3)–Ir(1)–Cl(4) 88.56(13), Cl(3)–Ir(2)–Cl(4) 88.13(13), Ir(1)–Cl(3)–Ir(2) 99.23(13), Ir(1)–Cl(4)–Ir(2) 98.71(12),

The geometry and bonding parameters of **11** (Figure 3) are analogous to those reported for related piano-stool complexes where Ir(III) is bonded to a C_5Me_5 ^{37–39} or a $\text{C}_5\text{Me}_4\text{Ph}$ ³⁵ ring, one chelating picolinato ligand and one terminal chloride. In particular, the replacement of one methyl substituent with a propyl one (compound **11**) on the cyclopentadienyl moiety does not determine any significant change in the distances between the iridium centre and the atoms bound to it.

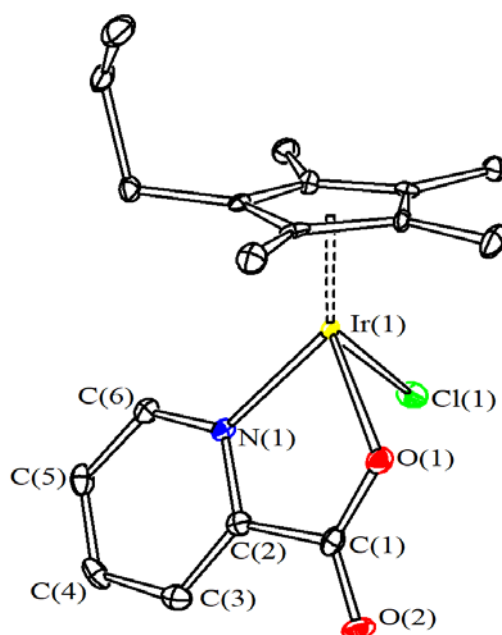


Figure 3. Molecular structure of $[\text{PrCp}^*\text{IrCl(pic)}]$, **11**. Displacement ellipsoids are at the 50% probability level. H-atoms have been omitted for clarity. Selected bond lengths (Å) and angles (°): Ir(1)–Cl(1) 2.4014(11), Ir(1)–N(1) 2.083(4), Ir(1)–O(1) 2.104(3), Ir(1)– PrCp^* 2.130(4)– 2.170(4), C(1)–O(1) 1.284(5), C(1)–O(2) 1.227(5), C(1)–C(2) 1.509(6), O(1)–Ir(1)–N(1) 77.43(13), Ir(1)–N(1)–C(2) 115.1(3), N(1)–C(2)–C(1) 115.0(3), C(2)–C(1)–O(1) 114.6(4), C(1)–O(1)–Ir(1) 116.9(3), C(2)–C(1)–O(2) 119.6(4), O(2)–C(1)–O(1) 125.8(4).

All complexes shown in Figure 1 exhibit high activity with TOF_{max} values included between 393 min^{-1} and 101 min^{-1} , depending on the nature and concentration of complex, and on the concentration of NaIO_4 (Tables 1 and 2). For each dimer, the orders in iridium and NaIO_4 were determined by varying the catalyst concentration (1, 2.5, 5, and 10 μM) at $[\text{NaIO}_4] = 20 \text{ mM}$ and the NaIO_4 concentration (5, 10, 20, 40 mM) at $[\text{Ir}] = 5 \mu\text{M}$, respectively. The orders in iridium and NaIO_4 are close to 1 and 0.5, respectively, for all catalysts (Supporting Information).

Six graphs are reported in the Supporting Information for each catalyst, showing: i) TON versus t at different catalyst concentrations; ii) TOF versus time at different catalyst concentrations; iii) TOF versus X at different catalyst concentrations; iv) TON versus t at different NaIO_4 concentrations; v)

This item was downloaded from IRIS Università di Bologna (<https://cris.unibo.it/>)

When citing, please refer to the published version.

TOF versus time at different NaIO_4 concentrations; and vi) TOF versus X at different NaIO_4 concentrations. An example of such graphs is reported in Figure 4 for the dimer **1**. Looking at the plots of Figure 4, and the analogous ones reported in the Supporting Information, it is immediately clear that dimers **1–9** act as extremely efficient WOCs. From TON versus t and TOF versus t trends, it is evident that all moles of O_2 expected, based on the amount of NaIO_4 used, are formed at every catalyst and NaIO_4 concentrations. TOF versus X plots are instead useful to graphically evaluate the order in catalyst according to reaction progress kinetic analysis (RPKA) proposed by Blackmond.^{40,41} For instance, because the TOF versus X plots at different catalyst concentration values show a substantial overlap (Figure 4 and Supporting Information), it can be immediately concluded that the reaction order in catalyst is 1. TOF versus X plots can also provide important information about the tendency of catalysts to activate.

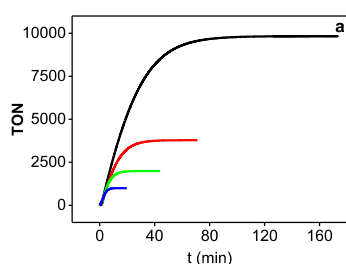


Figure 4: Kinetic trends for catalyst **1** (water solution at pH 7 by phosphate buffer 0.2 M, 25°C) at different iridium (a, b, c: black, 1 μM ; red, 2.5 μM ; green, 5 μM ; blue, 10 μM) and NaIO_4 (d, e, f: orange, 40 mM; green, 20 mM; violet, 10 mM; cyan, 5 mM) concentrations.

As stated above, the reaction yield is always close to 100% with $\text{TON}_{\text{max}} \approx 10000$. The dimeric complexes show the following relative scale of average TOF values (calculated on all the individual TOF values of the seven experiments carried out at different $[\text{Ir}]$ and $[\text{NaIO}_4]$): **2** (Me, 299 min^{-1}) \geq **3** (Et, 285 min^{-1}) \geq **1** (H, 260 min^{-1}) \geq **5** ($\text{CH}_2\text{CH}_2\text{NH}_2$, 244 min^{-1}) \approx **4** (nPr, 239 min^{-1}) \geq **9** (Bn, 216 min^{-1}) \geq **8** (4- $\text{C}_6\text{H}_4\text{OH}$, 193 min^{-1}) \approx **6** (Ph, 192 min^{-1}) \geq **7** (4- $\text{C}_6\text{H}_4\text{F}$, 177 min^{-1}). By comparing the blue series reported in Figure 5, in which the steric hindrance of R is varied, whereas its electronic contribution is approximately constant, it appears evident that the catalytic activity of dimers is significantly decreased when the steric hindrance of R increases. As a matter of fact, averaged TOF decreases from 299 min^{-1} for **2** (Me) down to 216 min^{-1} for **9** (Bn). It is also evident that less electron donating R substituents have a detrimental effect on the activity of dimers. Indeed, aryl-substituted Cp^* dimers (green in Figure 5) exhibit considerably lower averaged TOF values than alkyl substituted ones (blue in Figure 5). Interestingly, dimer **5** having a donating and potentially coordinating substituent ($\text{CH}_2\text{CH}_2\text{NH}_2$) behaves exactly as the isosteric complex **4** (nPr, red bar in Figure 5). Finally, the electronic factor appears to be predominant over the steric factor in **1** (H), which shows an average TOF (yellow bar in Figure 5) significantly lower than **2** (Me) and even **3** (Et).

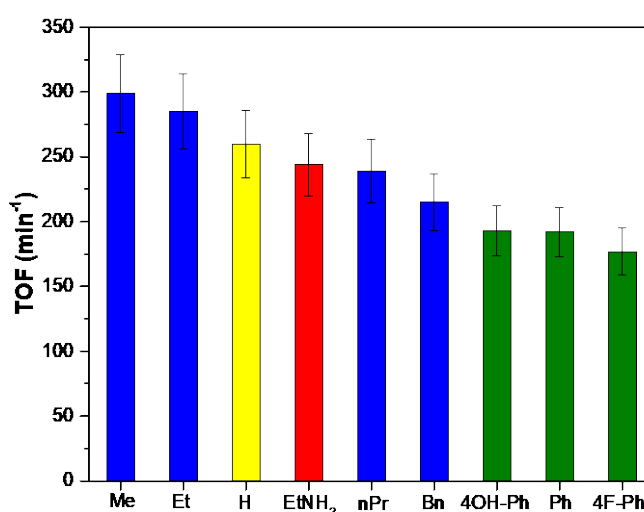


Figure 5. Average TOF values for NaIO₄ driven WO catalyzed by dimeric complexes **1-9** (water solution at pH 7 by phosphate buffer 0.2 M, 25°C, error bar = 10%).

Based on the results of previous studies, indicating, at least, a partial degradation of the Cp* ligand,²⁸ the observed catalytic trends can be interpreted in two different ways: i) a fragment of C₅Me₄R, still bearing the R-substituent, remains attached at iridium in the active species; ii) the active species is the same, independently of R, nevertheless the latter affects the achievement rate and/or the amount of the active species. If the first hypothesis were correct, it would be reasonable to conclude that an oxidative step of the water oxidation catalytic cycle is the turnover limiting step, since catalysis is favored by more electron donating substituents, and the achievement of the active species is an associative process, because it is disfavored by bulky substituents. In case the second hypothesis were correct, it could be presumed that more electron-donating C₅Me₄R groups might undergo faster oxidative transformation, since they are more strongly coordinated at iridium and, consequently, more activated toward oxygen attack, whereas bulkier substituents ask for more oxidative equivalents to be degraded, which are subtracted to catalysis, thus reducing the efficiency. In order to discriminate between these two hypotheses multiple injections consecutive catalytic experiments have been performed for the fastest (**2**_Me) and slowest (**7**_Ph_F) catalysts. The rationale underlying such an experiment is that if the active species is the same for all complexes (hypothesis ii)), the difference in the TOF of the two catalysts should become smaller and smaller or even vanish in runs successive to the first. The results are reported in Figure 6.

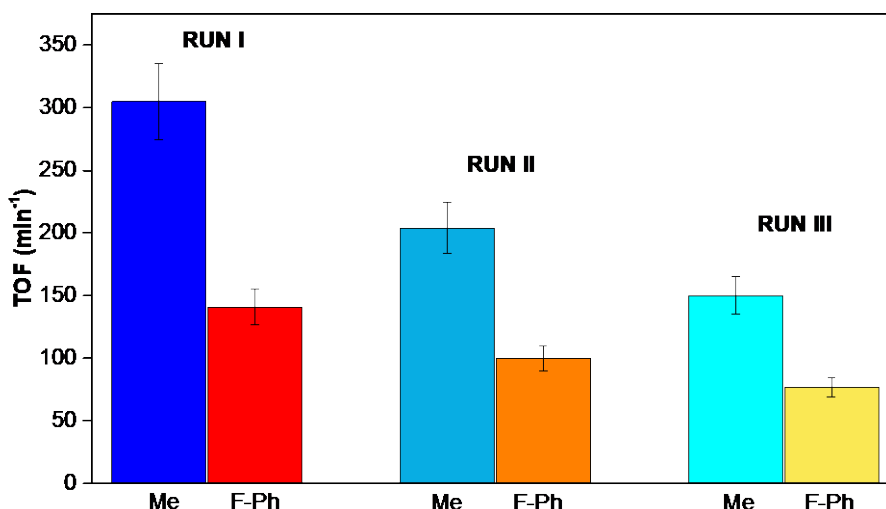


Figure 6. TOF values for NaIO₄ driven WO catalyzed by dimeric complexes **2** and **7** (water solution at pH 7 by phosphate buffer 0.2 M, 25°C, error bar = 10%) in triple run experiments.

Both **2** and **7** exhibit significant decrease of TOF passing from the first [**2**_Me, 305 ± 31 min⁻¹; **7**_Ph_F, 141 ± 14 min⁻¹] to the second [**2**_Me, 204 ± 20 min⁻¹; **7**_Ph_F, 100 ± 10 min⁻¹] and third [**2**_Me, 150 ± 15 min⁻¹; **7**_Ph_F, 79 ± 8 min⁻¹] run. Nevertheless, it is clear that their activity is not the same in each run. This finding supports hypothesis i). The observed reduced TOF in the second and third runs might be due to a decrease of the redox potential due to the presence of IO₃⁻, according to the Nernst equation ($E = E^0 - RT/nF \ln([IO_4^-]/[IO_3^-])$). Because TOF should be a function of ΔE (where $\Delta E = E - E^0 = -RT/nF \ln([IO_4^-]/[IO_3^-])$),⁴² this can be verified by plotting the measured TOF at any time as a function of ΔE for all three consecutive runs (Figure 7).

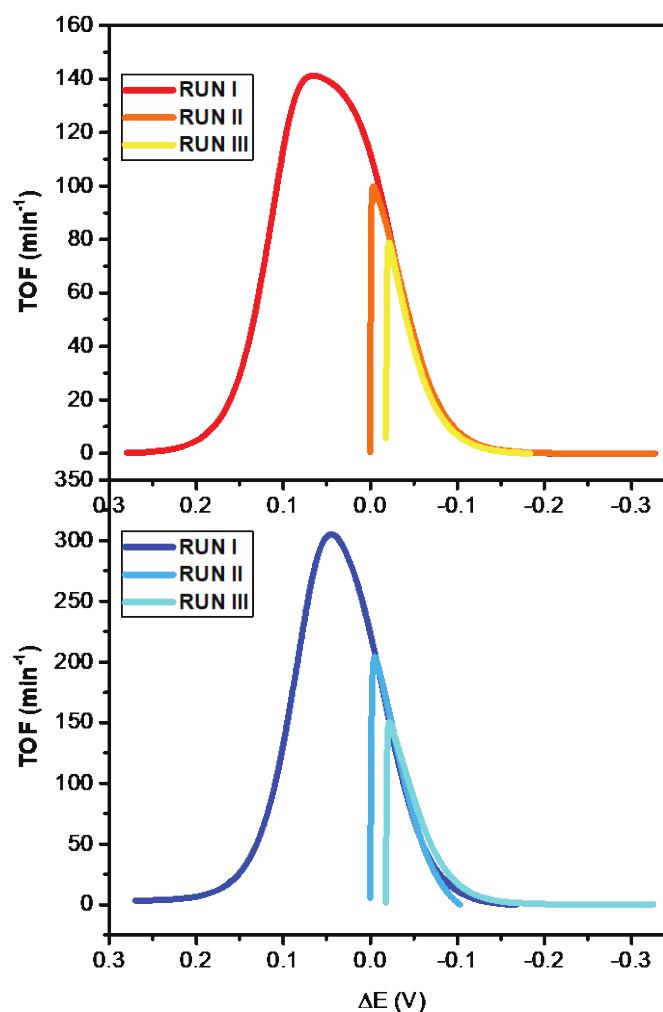


Figure 7. TOF *versus* ΔE for NaIO_4 driven WO catalyzed by the dimeric complex **2** (down) and **7** (top) (water solution at pH 7 by phosphate buffer 0.2 M, 25°C) in a triple run experiment showing that at the same redox potential TOF values are the same in all three experiments.

Before discussing the trends, it is important to outline that the initial decrease of ΔE from ca. 0.3 V down to the value corresponding to TOF_{MAX} , ca. 0.15 V, occurs very rapidly ($t_{\text{MAX}} = 1.6$ min and 2.5 min for **2** and **7**, respectively; $X_{\text{MAX}} = 0.13$ and 0.08 for **2** and **7**, respectively). Whereas the second part of the trends in Figure 7, from TOF_{MAX} on, is responsible for most of the reaction time. For example, $\Delta E = -0.1$ V is reached at $t = 16.9$ min and 30.3 min, for **2** and **7**, respectively ($X = 0.98$ for both precursors). It is reasonable to believe that during the initial growth of TOF a sort of

activation is occurring leading to the transformation of the precursors into the active species. Interestingly, after that period the three trends are perfectly coherent and the same TOF are observed for the three catalytic runs at the same potential value. This is a strong indication that the active species is the same during all the catalytic runs. The same coherent trends are observed for **7_Ph_F**, clearly with different TOF values with respect to those of **2_Me**. This means that also in this case the same active species is present in all three catalytic runs that, nevertheless, has to be different from that derived from **2_Me**. It seems reasonable to deduce that a fragment of R^{Cp}^* still containing R has to be present in the active species, consistently with hypothesis i). Another battery of experiments has been performed to enforce this hypothesis. Catalytic runs were carried out for **2_Me** at a definite initial redox potential injecting fresh catalyst into a water solution of a mixture of $\text{IO}_4^-/\text{IO}_3^-$. In such experiments the following concentrations were used: $[\text{IO}_4^-] = 20 \text{ mM}$ and $[\text{IO}_3^-] = 0 \text{ mM}, 1 \text{ mM}, 5 \text{ mM}, 10 \text{ mM}, 20 \text{ mM}, \text{ and } 40 \text{ mM}$. Furthermore, for each starting situation the second run (and in one case a third run) was also recorded. All catalytic experiments (first and second runs) are perfectly coherent in that exactly the same TOF is always observed at the same redox potential (Figure 8). Consistently, the same trends are observed for the successive runs and the ones with the fresh catalyst, when the initial $\text{IO}_4^-/\text{IO}_3^-$ ratio is the same.⁴³ This is, in our opinion, a clear demonstration that the active species must be always the same and should, consequently, contain a fragment of R^{Cp}^* still bearing R.

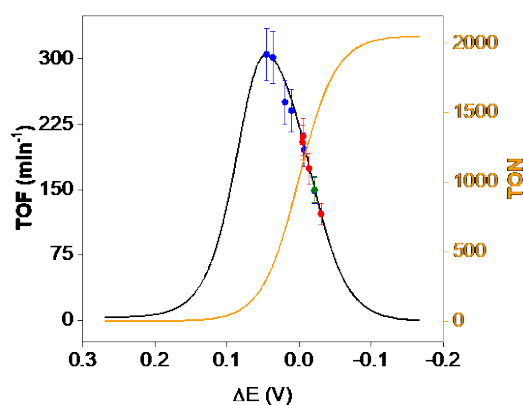


Figure 8. TOF (black) and TON (orange) *versus* ΔE trend for NaIO_4 (20 mM) driven WO catalyzed by the dimeric complex **2** (5 μM , water solution at pH 7 by phosphate buffer 0.2 M, 25°C). Blue (RUN I), red (RUN II) and green (RUN III) points represent the $\text{TOF}_{\text{MAX}}/\Delta E$ pair of values of independent catalytic runs carried out in the presence of variable amount of NaIO_3 .

3. CONCLUSIONS

4. EXPERIMENTAL SECTION

Synthesis and characterization of compounds

General details. Organic reactants were commercial products (TCI Europe or Merck) of the highest purity available. Solvents were purchased from Merck and, when required, distilled before use over appropriate drying agents. $\text{IrCl}_3 \cdot n\text{H}_2\text{O}$ was purchase from Merck. Compounds **2**,⁴⁴ **6**³⁴ and **9**³⁴ were prepared according to the respective literature procedures. Infrared spectra of solid samples were recorded on a Perkin Elmer Spectrum One FT-IR spectrometer, equipped with a UATR sampling accessory (4000-400 cm^{-1} range). UV-Vis spectra were recorded on an Ultraspec 2100 Pro spectrophotometer. IR and UV-Vis spectra were processed with Spectragryph software.⁴⁵ NMR spectra were recorded at 298 K on a Bruker Avance II DRX400 instrument equipped with a

BBFO broadband probe. Chemical shifts (expressed in parts per million) are referenced to the residual solvent peaks⁴⁶ (¹H, ¹³C) or to external standard (¹⁹F, CFCl₃). NMR spectra were assigned with the assistance of ¹H-¹³C (*gs*-HSQC and *gs*-HMBC) correlation experiments.⁴⁷ NMR signals due to a second isomeric form are italicized. Carbon, hydrogen and nitrogen analyses were performed on a Vario MICRO cube instrument (Elementar). Mass spectrometry measurements in positive ion scan mode were performed with an API 4000 instrument (SCIEX), equipped with an electrospray source.

C₅HMe₄(4-C₆H₄F). A solution of 2,3,4,5-tetramethyl-2-cyclopentenone (0.950 g, 1.09 mL, 6.87 mmol) in anhydrous THF (10 mL) was cooled down to -78 °C with a dry ice-acetone bath, then a solution of 4-fluorophenylmagnesium bromide (14.5 mL, 14.5 mmol) in THF was added dropwise. The mixture was stirred for 1 hour at -78 °C, and then allowed to warm to room temperature and stirred for additional 20 hours. The resulting reaction mixture was cooled to 0 °C and quenched with HCl (20 mL of a 1 M aqueous solution, 20 mmol). The obtained yellow solution was warmed to room temperature and stirred for 1 hour. The organic phase was washed with water (30 mL x 3), and dried over MgSO₄. The crude product was purified by alumina column chromatography, using pentane as eluent. A yellow solid was obtained upon solvent removal under vacuum. Yield: 0.577 g, 40%. IR (solid): $\tilde{\nu}/\text{cm}^{-1}$ = 3072w, 2919w, 1748w, 1484w-m, 1448m, 1379m, 1085m, 1020vs, 797m-s, 736w-m, 689w. ¹H NMR (CDCl₃): δ/ppm = 7.20, 7.07 (m, 4 H, C₆H₄), 3.17 (m, 1 H, MeCH), 2.02 (d, ⁴J_{HH} = 1.5 Hz, 3 H, CMe), 1.95, 1.89 (s, 6 H, CMe), 0.96 (d, 3 H, ³J_{HH} = 7.34 Hz, MeCH). ¹³C NMR (400 MHz, CDCl₃): δ/ppm = 161.0 (d, ¹J_{CF} = 244 Hz, CF), 141.7, 140.6, 137.1, 135.0 (CMe), 133.3 (C-C₅Me₄), 129.4 (d, ³J_{CF} = 7.4 Hz, C₆H₄), 115.0 (d, ²J_{CF} = 20.8 Hz, C₆H₄), 50.3 (CHMe), 14.5, 12.6, 11.9, 11.1 (CMe). ¹⁹F NMR (400 MHz, CDCl₃): δ/ppm = -115.7, -116.7,

–117.6. Isomer ratio ca. 1 : 1.5 : 32. Signals due to secondary isomeric forms are italicized. ESI-MS(+) $m/z = 217.1$ $[M+H]^+$.

C₅HMe₄(4-C₆H₄OH).³⁶ The title compound was obtained by using a modified literature procedure.³⁶ 2-Methoxypropene (3.0 mL, 0.031 mol) was added to 4-C₆H₄(Br)(OH) (2.63 g, 0.0152 mol), then a drop of POCl₃ was added to the mixture, which was allowed to stir at room temperature for 1 hour under protection from the light. Then few drops of NEt₃ were added, and the volatile materials were removed under reduced pressure. The resulting colourless oil, corresponding to 1,4-C₆H₄(Br)(OCMe₂OMe), was dissolved in Et₂O (20 mL) under nitrogen atmosphere. The solution was cooled to ca. –70 °C, and a 2.5 M solution of butyllithium in hexanes (6.0 mL, 0.015 mol) was added dropwise. The solution was stirred for 90 min during which time it was allowed to warm to room temperature. The final mixture was cooled to ca. –70°C and treated dropwise with 2,3,4,5-tetramethyl-2-cyclopentenone (2.3 mL, 0.015 mol) under nitrogen atmosphere. The resulting yellow solution was stirred overnight, then it was quenched with H₂O (2 mL). A yellow mixture was obtained which was stirred for additional 10 minutes. The liquid was separated, and the residue was washed with Et₂O (2 x 20 mL) in order to extract more organic substrate. The collected organic phases were eliminated of the volatiles under vacuum, thus affording a dark brown oil, which was dried over P₂O₅ overnight. Yield: 2.70 g, 83% respect to 4-C₆H₄(Br)(OH). ¹H NMR (400 MHz, CDCl₃): δ /ppm = 7.11, 6.89 (d, 2 H, ³J_{HH} = 8.31 Hz, C₆H₄), 4.93 (br, 1 H, OH), 3.13 (m, 1 H, MeCH), 2.00, 1.93, 1.86 (s, 9 H, CMe), 0.94 (d, 3 H, ³J_{HH} = 7.83 Hz, MeCH).

C₅HMe₄(4-C₆H₄OCMe₂OMe).³⁶ C₅HMe₄(4-C₆H₄OH) (2.05 g, 9.57 mmol) was treated with 2-methoxypropene (1.8 mL, 19 mol), then a drop of POCl₃ was added to the mixture. The resulting mixture was allowed to stir at room temperature for 1 hour, and then quenched with five drops of NEt₃. Removal of the volatiles under reduced pressure afforded an orange-brown oil, which was

purified by filtration through an alumina column using Et₂O as eluent. Yield: 2.32 g, 85%. ¹H NMR (400 MHz, CDCl₃): δ/ppm = 7.17, 7.15 (d, 2 H, C₆H₄); 3.47 (s, 3 H, OMe); 3.15 (m, 1 H, MeCH); 2.03, 1.94, 1.88 (s, 9 H, CMe); 1.52 (s, 6 H, CMe₂); 0.97 (d, 3 H, ³J_{HH} = 7.34 Hz, MeCH).

[^HCp*IrCl(μ-Cl)]₂ (**1**). A solution of tetramethylcyclopentadiene (0.38 mL, 2.1 mmol) and IrCl₃·nH₂O (54.6% of Ir, 0.500 g, 1.42 mmol) in degassed MeOH (20 mL) was heated at reflux for 48 hours. Then the resulting mixture was allowed to cool to room temperature, concentrated under reduced pressure and stored at -30 °C for 24 hours. An orange precipitate was recovered, washed with cold methanol and diethyl ether and dried under vacuum. Yield: 0.128 g, 23%. Anal. calcd. for C₁₈H₂₆Cl₄Ir₂: C, 28.13; H, 3.41. Found: C, 28.21; H, 3.50. IR (solid): $\tilde{\nu}/\text{cm}^{-1}$ = 3072w, 2919w, 1748w, 1484w-m, 1448m, 1379m, 1085m, 1020vs, 797m-s, 736w-m, 689w. ¹H NMR (400 MHz, CDCl₃): δ/ppm = 5.30 (s, 1 H, C₅Me₄H), 1.70, 1.65 (s, 12 H, Me). ¹³C NMR (400 MHz, CDCl₃): δ/ppm = 91.8, 86.3 (CMe), 68.1 (CH), 11.0, 9.3 (CMe). ESI-MS(+) *m/z* = 733.0 [M-Cl]⁺.

[^{Et}Cp*IrCl(μ-Cl)]₂ (**3**). A solution of tetramethyl(ethyl)cyclopentadiene (0.31 mL, 1.8 mmol) and IrCl₃·nH₂O (54.6% of Ir, 0.400 g, 1.17 mmol) in degassed MeOH (20 mL) was heated at reflux for 48 hours. The resulting mixture was allowed to cool to room temperature, filtered to eliminate some dark solid, and concentrated under reduced pressure. The crude product was purified by washing with diethyl ether (2 x 20 mL) and subsequent crystallization from a double layer CH₂Cl₂/hexane at -30 °C, affording an orange solid. Yield: 0.142 g, 30%. Anal. calcd. for C₂₂H₃₄Cl₃Ir₂: C, 33.46; H, 4.31. Found: C, 33.28; H, 4.33. IR (solid): $\tilde{\nu}/\text{cm}^{-1}$ = 2965m, 2905w-m, 2115m, 1995w-m, 1456vs, 1379s, 1158w, 1088w, 1056m, 1030vs, 968m, 825w, 735w-m. ¹H NMR (400 MHz, CDCl₃): δ/ppm = 2.18 (q, ³J_{HH} = 7.7 Hz, 2 H, CH₂), 1.61, 1.59 (s, 12 H, CMe), 1.11 (t, ³J_{HH} = 7.7 Hz, 3 H, CH₂CH₃). ¹³C NMR (400 MHz, CDCl₃): δ/ppm = 89.1 (CEt), 86.5, 86.2 (CMe), 17.6 (CH₂), 11.7 (CH₂CH₃), 9.3, 9.2 (CMe). ESI-MS(+) *m/z* = 789.3 [M-Cl]⁺.

$[\text{PrCp}^*\text{IrCl}(\mu\text{-Cl})]_2$ (**4**). The title compound was obtained by using a procedure analogous to that described for the synthesis of **3**, from tetramethyl(propyl)cyclopentadiene (0.43 mL, 2.1 mmol) and $\text{IrCl}_3 \cdot n\text{H}_2\text{O}$ (54.6% of Ir, 0.500 g, 1.42 mmol). Orange solid, yield: 0.152 g, 20%. Anal. calcd. for $\text{C}_{24}\text{H}_{38}\text{Cl}_4\text{Ir}_2$: C, 33.80; H, 4.46. Found: C, 33.67; H, 4.52. IR (solid): $\tilde{\nu}/\text{cm}^{-1} = 2963\text{m-s}, 2913\text{m}, 2837\text{w}, 1450\text{vs}, 1381\text{s}, 1226\text{w}, 1153\text{w}, 1086\text{m}, 1029\text{vs}, 818\text{m-s}, 760\text{m}, 673\text{m-s}$. ^1H NMR (400 MHz, CDCl_3): $\delta/\text{ppm} = 2.15, 1.47$ (m, 4 H, CH_2), 1.61, 1.59 (s, 12 H, CMe), 0.96 (t, $^3J_{\text{HH}} = 7.4$ Hz, 3 H, CH_2CH_3). ^{13}C NMR (400 MHz, CDCl_3): $\delta/\text{ppm} = 87.9$ (CPr), 86.5 (CMe), 26.1, 20.9 (CH_2), 14.27 (CH_2CH_3), 9.5, 9.4 (CMe). ESI-MS(+) $m/z = 817.3$ $[\text{M-Cl}]^+$.

$[\text{CH}_2\text{CH}_2\text{NH}_2\text{Cp}^*\text{IrCl}(\mu\text{-Cl})]_2$ (**5**). XXX

$[\text{4F-PhCp}^*\text{IrCl}(\mu\text{-Cl})]_2$ (**7**). The title compound was obtained by using a procedure analogous to that described for the synthesis of **3**, from 4-floro-(2,3,4,5-tetramethylcyclopenta-2,4-dien-1-yl)benzene (0.463 g, 2.14 mmol) and $\text{IrCl}_3 \cdot n\text{H}_2\text{O}$ (54.6% of Ir, 0.503 g, 1.43 mmol). The crude product was purified by washing with pentane (2 x 20 mL) and subsequent crystallization from a double layer CH_2Cl_2 /pentane at -30 °C, affording a dark yellow solid. Yield: 0.294 g, 43%. Anal. calcd. for $\text{C}_{30}\text{H}_{32}\text{Cl}_4\text{F}_2\text{Ir}_2$: C, 37.66; H, 3.35. Found: C, 37.40; H, 3.47. IR (solid): $\tilde{\nu}/\text{cm}^{-1} = 3072\text{w}, 2992\text{w}, 2952\text{w}, 2915\text{w}, 2774\text{w-m}, 2058\text{m}, 1985\text{w}, 1607\text{m-s}, 1518\text{vs}, 1458$ m-s, 1394w, 1380m-s, 1301w-m, 1227s, 1159s, 1097w-m, 1027m, 994m, 848s, 818s, 743m-w, 721w-m, 676m, 669m. ^1H NMR (400 MHz, CDCl_3): $\delta/\text{ppm} = 7.57$ (dd, $^4J_{\text{HF}} = 5.20$ Hz, $^3J_{\text{HH}} = 8.31$ Hz, 2 H, C_6H_4), 7.04 (t, $^3J_{\text{HF}} = 8.31$ Hz, $^3J_{\text{HH}} = 8.31$ Hz, 2 H, C_6H_4), 1.71, 1.60 (s, 12 H, Me). ^{13}C NMR (400 MHz, CDCl_3): $\delta/\text{ppm} = 162.9$ (d, $^1J_{\text{CF}} = 248$ Hz, CF), 132.2 (d, $^3J_{\text{CF}} = 8.9$ Hz, C_6H_4), 115.9 (d, $^2J_{\text{CF}} = 22.3$ Hz, C_6H_4), 125.7 ($\text{C-C}_5\text{Me}_4$), 93.6, 85.7 (CMe), 81.4 ($\text{C-C}_6\text{H}_4$), 10.3, 9.6 (CMe). ^{19}F NMR (400 MHz, CDCl_3): $\delta/\text{ppm} = -112.7$. ESI-MS(+) $m/z = 921.3$ $[\text{M-Cl}]^+$. Crystals of **7** suitable for X-ray analysis were obtained from a concentrated CDCl_3 solution stored at -30 °C.

$[\text{HO-PhCp}^*\text{IrCl}(\mu\text{-Cl})_2]$ (**8**). A solution of $\text{C}_5\text{HMe}_4(4\text{-C}_6\text{H}_4\text{OCMe}_2\text{OMe})$ (400 mg, 1.40 mmol) and $\text{IrCl}_3 \cdot 3\text{H}_2\text{O}$ (350 mg, 0.993 mmol) in degassed MeOH (30 mL) was heated at reflux for 72 h under N_2 atmosphere. Afterwards, the reaction mixture was allowed to cool to room temperature, and the volatiles were removed under reduced pressure. The resulting brown oil was charged on a silica column; after elimination of undesired substances with hexane/ Et_2O mixtures, an orange fraction was collected by using a mixture of diethyl ether and acetone (1:1 v/v) as eluent. The product was obtained as an orange solid upon removal of the volatile materials under vacuum. Yield: 0.142 g, 30%. Anal. calcd. for $\text{C}_{30}\text{H}_{34}\text{Cl}_4\text{Ir}_2\text{O}_2$: C, 37.82; H, 3.60. Found: C, 37.56; H, 3.51. IR (solid): $\tilde{\nu}/\text{cm}^{-1} = 3305\text{m} (\nu_{\text{OH}})$, 2921w, 1611m, 1590w, 1519s, 1499w, 1446m, 1376w, 1365w, 1346w, 1265s, 1211m-s, 1173s, 1103w-m, 1031m, 994w, 850vs, 818s, 761m-s, 692m. ^1H NMR (400 MHz, CD_3OD): $\delta/\text{ppm} = 7.45$ (d, 2 H, $^3J_{\text{HH}} = 8.3$ Hz, C_6H_4), 6.81 (d, 2 H, $^3J_{\text{HH}} = 8.8$ Hz, C_6H_4), 1.68, 1.61 (s, 12 H, CMe). ^{13}C NMR (400 MHz, CD_3OD): $\delta = 157.9$ (COH), 131.3, 115.0 (C_6H_4), 120.0 (C- C_5Me_4), 93.2, 85.2 (CMe), 78.1 (C- C_6H_4), 9.1, 8.2 (CMe). ESI-MS(+) $m/z = 952.8$ $[\text{M-Cl}]^+$.

$[\text{H}^*\text{Cp}^*\text{IrCl}(\text{pic})]_2$. **1** (0.128 g, 0.166 mmol), 2-pyridinecarboxylic acid (0.048 g, 0.383 mmol) and sodium methoxide (0.021 g, 0.383 mmol) were dissolved in MeOH (20 mL) in the order given. The mixture was refluxed for 3 hours. Afterwards, the solvent was removed and the crude product was extracted with $\text{CH}_2\text{Cl}_2/\text{H}_2\text{O}$. The organic phase was dried over Na_2SO_4 , filtered and concentrated under reduced pressure affording **11** as a yellow solid. Yield: 0.062 g, 40%. Anal. calcd. for $\text{C}_{15}\text{H}_{17}\text{IrNO}_2$: C, 41.37; H, 3.93. Found: C, 41.44; H, 4.00. IR (solid): $\tilde{\nu}/\text{cm}^{-1} = 1651\text{vs}$, 1602m-s, 1568w, 1494w-m, 1469w-m, 1441m, 1385w, 1338s, 1304w-m, 1285m, 1264m, 1247m, 1166w-m, 1097m, 1053m, 1029m-s, 849m, 835m, 806m, 787s, 735w-m, 709m, 693m-s, 655 m. ^1H NMR (400 MHz, dmsO-d_6): $\delta/\text{ppm} = 8.98$, 8.16, 7.93, 7.78 (m, 4 H, $\text{C}_5\text{H}_4\text{N}$), 5.57 (s, 1 H, $\text{C}_5\text{Me}_4\text{H}$), 1.73, 1.67, 1.64, 1.63 (s, 12 H, Me). ^{13}C NMR (400 MHz, dmsO-d_6): $\delta/\text{ppm} = 172.8$ (OCO), 152.3, 150.6,

140.4, 129.7, 126.9 (C₅H₄N), 92.8, 91.0, 86.7, 83.5 (CMe), 67.1 (CH), 10.6, 10.3, 8.9, 8.8 (CMe). ESI-MS(+) m/z = 436.0 [M-Cl]⁺.

[^{Pr}Cp*IrCl(pic)]₂ (**12**). The title compound was prepared by the same procedure as that described for the synthesis of **11**, from **4** (0.111 g, 0.130 mmol), 2-pyridinecarboxylic acid (0.039 g, 0.316 mmol) and sodium methoxide (0.017 g, 0.315 mmol). Yellow solid, yield: 0.101 g, 76%. Anal. calcd. for C₁₈H₂₃ClIrNO₂: C, 42.14; H, 4.52. Found: C, 42.02; H, 4.58. IR (solid): $\tilde{\nu}/\text{cm}^{-1}$ = 2876w, 1661v-s, 1605m, 1568w, 1495w, 1469m-w, 1456m-w, 1384m-w, 1338s, 1286m, 1244m-w, 1170m, 1112w, 1096m-w, 1056m-w, 1035m, 991w, 960w, 917w, 917m-w, 847m, 827m, 816m-w, 775s, 733w, 706m, 692m, 674 m-w, 658w cm⁻¹. ¹H NMR (400 MHz, CDCl₃): δ/ppm = 8.57, 8.17, 7.95, 7.57 (m, 4 H, C₅H₄N), 2.12 (td, 2 H, J_{HH} = 7.5 and 4.2 Hz, CH₂), 1.72, 1.71 (s, 12 H, CMe), 1.51 (dq, 2 H, J_{HH} = 15.1 and 7.5 Hz, CH₂), 0.97 (t, 3 H, ³J_{HH} = 7.5 Hz, CH₂CH₃). ¹³C NMR (400 MHz, CDCl₃): δ/ppm = 172.9 (OCO), 151.1, 149.5, 139.3, 128.8, 127.6 (C₅H₄N), 86.9, 86.5, 86.0, 85.6 (CMe), 25.9, 21.5 (CH₂), 14.2 (CH₂CH₃), 9.1, 9.0 (CMe). ESI-MS(+) m/z = 478.0 [M-Cl]⁺. Crystals suitable for X-ray analysis were obtained from a dichloromethane solution layered with hexane and stored at -30 °C for one week.

X-ray crystallography. Crystal data and collection details for **7** and **11** are reported in Table 3. Data were recorded on a Bruker APEX II diffractometer equipped with a PHOTON2 detector using Mo-K α radiation. Data were corrected for Lorentz polarization and absorption effects (empirical absorption correction SADABS).[G. M. Sheldrick, SADABS-2008/1 - Bruker AXS Area Detector Scaling and Absorption Correction, Bruker AXS: Madison, Wisconsin, USA, 2008] The structure was solved by direct methods and refined by full-matrix least-squares based on all data using F^2 .⁴⁸ The crystals of **7** appeared to be nonmerohedrally twinned. The TwinRotMat routine of PLATON (A. L. Spek, PLATON, A Multipurpose Crystallographic Tool; Utrecht University: Utrecht, The

This item was downloaded from IRIS Università di Bologna (<https://cris.unibo.it/>)

When citing, please refer to the published version.

Netherlands, 2005)) was used to determine the twinning matrix and to write the reflection data file (.hkl) containing the two twin components. Refinement was performed using the instruction HKLF 5 in SHELXL and one BASF parameter, which refined as 0.603(16).

The crystals of **11** are racemically twinned with refined Flack parameter 0.394(7).⁴⁹

Hydrogen atoms were fixed at calculated positions and refined by a riding model. All non-hydrogen atoms were refined with anisotropic displacement parameters.

Table 3. Crystal data and measurement details for **7** and **11**.

	7	11
Formula	C ₁₈ H ₂₃ ClIrNO ₂	C ₃₀ H ₃₂ Cl ₄ F ₂ Ir ₂
FW	513.02	956.75
T, K	100(2)	100(2)
λ , Å	0.71073	0.71073
Crystal system	Orthorhombic	Triclinic
Space group	<i>P</i> 2 ₁ 2 ₁ 2 ₁	<i>P</i> $\bar{1}$ 2
<i>a</i> , Å	8.2268(3)	8.7487(10)
<i>b</i> , Å	14.3426(6)	17.713(2)
<i>c</i> , Å	14.5746(6)	20.308(3)
α , °	90	73.261(4)
β , °	90	89.913(4)
γ , °	90	83.794(4)
Cell Volume, Å ³	1740.95(12)	2994.6(6)
Z	4	4
<i>D</i> _c , g·cm ⁻³	1.957	2.122
μ , mm ⁻¹	7.831	9.267
F(000)	922	1808
Crystal size, mm	0.21×0.18×0.14	0.25×0.18×0.11
θ limits, °	1.980-26.998	1.814-24.999
Reflections collected	25212	40544
Independent reflections	3816 [<i>R</i> _{int} = 0.0371]	10506 [<i>R</i> _{int} = 0.0808]
Data / restraints / parameters	3816 / 0 / 214	10506 / 451 / 694
Goodness on fit on F ²	1.189	1.074
<i>R</i> ₁ (<i>I</i> > 2 σ (<i>I</i>))	0.0145	0.0612
<i>wR</i> ₂ (all data)	0.0330	0.1479
Absolute structure parameter	0.394(7)	-
Largest diff. peak and hole, e Å ⁻³	0.615 / -0.892	3.229 / -3.698

ASSOCIATED CONTENT

(Word Style “TE_Supporting_Information”). **Supporting Information.** A listing of the contents of each file supplied as Supporting Information should be included. For instructions on what should be

This item was downloaded from IRIS Università di Bologna (<https://cris.unibo.it/>)

When citing, please refer to the published version.

included in the Supporting Information as well as how to prepare this material for publications, refer to the journal's Instructions for Authors.

The following files are available free of charge.

brief description (file type, i.e., PDF)

brief description (file type, i.e., PDF)

CCDC reference numbers 2014602 (**7**) and 1953420 (**11**) contain the supplementary crystallographic data for the X-ray studies reported in this paper. These data can be obtained free of charge at www.ccdc.cam.ac.uk/conts/retrieving.html (or from the Cambridge Crystallographic Data Centre, 12, Union Road, Cambridge CB2 1EZ, UK; fax: (internat.) +44-1223/336-033; e-mail: deposit@ccdc.cam.ac.uk).

AUTHOR INFORMATION

Corresponding Author

*(Word Style "FA_Corresponding_Author_Footnote"). * (Word Style "FA_Corresponding_Author_Footnote"). Give contact information for the author(s) to whom correspondence should be addressed.

Author Contributions

The manuscript was written through contributions of all authors. All authors have given approval to the final version of the manuscript. ‡These authors contributed equally. (match statement to author names with a symbol)

Notes

Any additional relevant notes should be placed here.

This item was downloaded from IRIS Università di Bologna (<https://cris.unibo.it/>)

When citing, please refer to the published version.

ACKNOWLEDGMENT

(Word Style “TD_Acknowledgments”). Generally the last paragraph of the paper is the place to acknowledge people, organizations, and financing (you may state grant numbers and sponsors here). Follow the journal’s guidelines on what to include in the Acknowledgments section.

REFERENCES

- (1) Alstrum-Acevedo, J. H.; Brennaman, M. K.; Meyer, T. J. Chemical Approaches to Artificial Photosynthesis. 2. *Inorg. Chem.* **2005**, *44* (20), 6802–6827 DOI: 10.1021/ic050904r.
- (2) Lewis, N. S.; Nocera, D. G. Powering the planet: Chemical challenges in solar energy utilization. *Proc. Natl. Acad. Sci.* **2006**, *103* (43), 15729 LP – 15735 DOI: 10.1073/pnas.0603395103.
- (3) Balzani, V.; Credi, A.; Venturi, M. Photochemical conversion of solar energy. *ChemSusChem* **2008**, *1* (1–2), 26–58 DOI: 10.1002/cssc.200700087.
- (4) Gust, D.; Moore, T. A.; Moore, A. L. Solar Fuels via Artificial Photosynthesis. *Acc. Chem. Res.* **2009**, *42* (12), 1890–1898 DOI: 10.1021/ar900209b.
- (5) McDaniel, N. D.; Bernhard, S. Solar fuels: thermodynamics, candidates, tactics, and figures of merit. *Dalt. Trans.* **2010**, *39* (42), 10021–10030 DOI: 10.1039/C0DT00454E.
- (6) Berardi, S.; Drouet, S.; Francàs, L.; Gimbert-Suriñach, C.; Guttentag, M.; Richmond, C.; Stoll, T.; Llobet, A. Molecular artificial photosynthesis. *Chem. Soc. Rev.* **2014**, *43* (22), 7501–7519 DOI: 10.1039/C3CS60405E.
- (7) Kanan, M. W.; Nocera, D. G. In Situ Formation of an Water Containing Phosphate and Co 2 +. *Science* (80-.). **2008**, *321* (August), 1072–1075 DOI: 10.1126/science.1162018.
- (8) Wang, C.; Wang, J.-L. L.; Lin, W. Elucidating Molecular Iridium Water Oxidation Catalysts Using

This item was downloaded from IRIS Università di Bologna (<https://cris.unibo.it/>)

When citing, please refer to the published version.

Metal-Organic Frameworks: A Comprehensive Structural, Catalytic, Spectroscopic, and Kinetic Study.

J. Am. Chem. Soc. **2012**, *134* (48), 19895–19908 DOI: 10.1021/ja310074j.

- (9) McCrory, C. C. L.; Jung, S. H.; Peters, J. C.; Jaramillo, T. F. Benchmarking Heterogeneous Electrocatalysts for the Oxygen Evolution Reaction. *J. Am. Chem. Soc.* **2013**, *135* (45), 16977–16987 DOI: 10.1021/ja407115p.
- (10) Chen, Z.; Concepcion, J. J.; Hu, X.; Yang, W.; Hoertz, P. G.; Meyer, T. J. Concerted O atom-proton transfer in the O-O bond forming step in water oxidation. *Proc. Natl. Acad. Sci. U. S. A.* **2010**, *107* (16), 7225–7229 DOI: 10.1073/pnas.1001132107.
- (11) Savini, A.; Bucci, A.; Nocchetti, M.; Vivani, R.; Idriss, H.; Macchioni, A. Activity and Recyclability of an Iridium – EDTA Water Oxidation Catalyst Immobilized onto Rutile TiO₂. *ACS Catal.* **2015**, *5*, 264–271.
- (12) Pastori, G.; Wahab, K.; Bucci, A.; Bellachioma, G.; Zuccaccia, C.; Llorca, J.; Idriss, H.; Macchioni, A. Heterogenized Water Oxidation Catalysts Prepared by Immobilizing Kläui-Type Organometallic Precursors. *Chem. - A Eur. J.* **2016**, *22* (38), 13459–13463 DOI: 10.1002/chem.201602008.
- (13) Materna, K. L.; Rudshteyn, B.; Brennan, B. J.; Kane, M. H.; Bloomfield, A. J.; Huang, D. L.; Shopov, D. Y.; Batista, V. S.; Crabtree, R. H.; Brudvig, G. W. Heterogenized Iridium Water-Oxidation Catalyst from a Silatrane Precursor. *ACS Catal.* **2016**, *6* (8), 5371–5377 DOI: 10.1021/acscatal.6b01101.
- (14) Materna, K. L.; Crabtree, R. H.; Brudvig, G. W. Anchoring groups for photocatalytic water oxidation on metal oxide surfaces. *Chem. Soc. Rev.* **2017**, *46* (20), 6099–6110 DOI: 10.1039/C7CS00314E.
- (15) Wan, X.; Wang, L.; Dong, C.-L.; Menendez Rodriguez, G.; Huang, Y.-C.; Macchioni, A.; Shen, S. Activating Kläui-Type Organometallic Precursors at Metal Oxide Surfaces for Enhanced Solar Water Oxidation. *ACS Energy Lett.* **2018**, *3*, 1613–1619 DOI: 10.1021/acsenergylett.8b00847.

This item was downloaded from IRIS Università di Bologna (<https://cris.unibo.it/>)

When citing, please refer to the published version.

- (16) Duan, L.; Bozoglian, F.; Mandal, S.; Stewart, B.; Privalov, T.; Llobet, A.; Sun, L. A molecular ruthenium catalyst with water-oxidation activity comparable to that of photosystem II. *Nat. Chem.* **2012**, *4* (5), 418–423 DOI: 10.1038/nchem.1301.
- (17) Llobet, A. *Molecular Water Oxidation Catalysis*; Llobet, A., Ed.; Wiley, 2014.
- (18) Creus, J.; Matheu, R.; Peñafiel, I.; Moonshiram, D.; Blondeau, P.; Benet-Buchholz, J.; García-Antón, J.; Sala, X.; Godard, C.; Llobet, A. A Million Turnover Molecular Anode for Catalytic Water Oxidation. *Angew. Chemie - Int. Ed.* **2016**, *55* (49), 15382–15386 DOI: 10.1002/anie.201609167.
- (19) Gerlach, D. L.; Bhagan, S.; Cruce, A. A.; Burks, D. B.; Nieto, I.; Truong, H. T.; Kelley, S. P.; Herbst-Gervasoni, C. J.; Jernigan, K. L.; Bowman, M. K.; et al. Studies of the pathways open to copper water oxidation catalysts containing proximal hydroxy groups during basic electrocatalysis. *Inorg. Chem.* **2014**, *53* (24), 12689–12698 DOI: 10.1021/ic501018a.
- (20) Fillol, J. L.; Codolà, Z.; Garcia-Bosch, I.; Gàmez, L.; Pla, J. J.; Costas, M. Efficient water oxidation catalysts based on readily available iron coordination complexes. *Nat. Chem.* **2011**, *3* (10), 807–813 DOI: 10.1038/nchem.1140.
- (21) Silva, P.; Vilela, S. M. F.; Tomé, J. P. C.; Almeida Paz, F. A. Multifunctional metal–organic frameworks: from academia to industrial applications. *Chem. Soc. Rev.* **2015**, *44* (19), 6774–6803 DOI: 10.1039/C5CS00307E.
- (22) Corbucci, I.; Albrecht, A. M. M. Iridium Complexes in Water Oxidation Catalysis. In *Iridium(III) in Optoelectronic and Photonics Applications*; 2017.
- (23) Macchioni, A. The Middle-Earth between Homogeneous and Heterogeneous Catalysis in Water Oxidation with Iridium. *Eur. J. Inorg. Chem.* **2019**, *2019* (1), 7–17 DOI: 10.1002/ejic.201800798.

This item was downloaded from IRIS Università di Bologna (<https://cris.unibo.it/>)

When citing, please refer to the published version.

- (24) Blakemore, J. D.; Schley, N. D.; Balcells, D.; Hull, J. F.; Olack, G. W.; Incarvito, C. D.; Eisenstein, O.; Brudvig, G. W.; Crabtree, R. H. Half-sandwich iridium complexes for homogeneous water-oxidation catalysis. *J. Am. Chem. Soc.* **2010**, *132* (45), 16017–16029 DOI: 10.1021/ja104775j.
- (25) Savini, A.; Belanzoni, P.; Bellachioma, G.; Zuccaccia, C.; Zuccaccia, D.; Macchioni, A. Activity and degradation pathways of pentamethyl-cyclopentadienyl-iridium catalysts for water oxidation. *Green Chem.* **2011**, *13* (12), 3360–3374 DOI: 10.1039/c1gc15899f.
- (26) Grotjahn, D. B.; Brown, D. B.; Martin, J. K.; Marelius, D. C.; Abadjian, M. C.; Tran, H. N.; Kalyuzhny, G.; Vecchio, K. S.; Specht, Z. G.; Cortes-Llamas, S. A.; et al. Evolution of iridium-based molecular catalysts during water oxidation with ceric ammonium nitrate. *J. Am. Chem. Soc.* **2011**, *133* (47), 19024–19027 DOI: 10.1021/ja203095k.
- (27) Zuccaccia, C.; Bellachioma, G.; Bolaño, S.; Rocchigiani, L.; Savini, A.; Macchioni, A. An NMR study of the oxidative degradation of Cp*Ir catalysts for water oxidation: Evidence for a preliminary attack on the quaternary carbon atom of the -C-CH₃ moiety. *Eur. J. Inorg. Chem.* **2012**, *2* (9), 1462–1468 DOI: 10.1002/ejic.201100954.
- (28) Zuccaccia, C.; Bellachioma, G.; Bortolini, O.; Bucci, A.; Savini, A.; Macchioni, A. Transformation of a Cp*-iridium(III) precatalyst for water oxidation when exposed to oxidative stress. *Chem. - A Eur. J.* **2014**, *20* (12), 3446–3456 DOI: 10.1002/chem.201304412.
- (29) Menendez Rodriguez, G.; Bucci, A.; Hutchinson, R.; Bellachioma, G.; Zuccaccia, C.; Giovagnoli, S.; Idriss, H.; Macchioni, A. Extremely Active, Tunable, and pH-Responsive Iridium Water Oxidation Catalysts. *ACS Energy Lett.* **2017**, *2* (1), 105–110 DOI: 10.1021/acsenenergylett.6b00606.
- (30) Hintermair, U.; Sheehan, S. W.; Parent, A. R.; Ess, D. H.; Richens, D. T.; Vaccaro, P. H.; Brudvig, G. W.; Crabtree, R. H. Precursor transformation during molecular oxidation catalysis with organometallic

This item was downloaded from IRIS Università di Bologna (<https://cris.unibo.it/>)

When citing, please refer to the published version.

iridium complexes. *J. Am. Chem. Soc.* **2013**, *135* (29), 10837–10851 DOI: 10.1021/ja4048762.

- (31) Ingram, A. J.; Wolk, A. B.; Flender, C.; Zhang, J.; Johnson, C. J.; Hintermair, U.; Crabtree, R. H.; Johnson, M. A.; Zare, R. N. Modes of activation of organometallic iridium complexes for catalytic water and C-H oxidation. *Inorg. Chem.* **2014**, *53* (1), 423–433 DOI: 10.1021/ic402390t.
- (32) Yang, K. R.; Matula, A. J.; Kwon, G.; Hong, J.; Sheehan, S. W.; Thomsen, J. M.; Brudvig, G. W.; Crabtree, R. H.; Tiede, D. M.; Chen, L. X.; et al. Solution structures of highly active molecular ir water-oxidation catalysts from density functional theory combined with high-energy X-ray scattering and EXAFS spectroscopy. *J. Am. Chem. Soc.* **2016**, *138* (17), 5511–5514 DOI: 10.1021/jacs.6b01750.
- (33) Rodriguez, G. M.; Gatto, G.; Zuccaccia, C.; Macchioni, A. Benchmarking Water Oxidation Catalysts Based on Iridium Complexes: Clues and Doubts on the Nature of Active Species. *ChemSusChem* **2017**, *10* (22), 4503–4509 DOI: doi:10.1002/cssc.201701818.
- (34) Morris, D. M.; McGeagh, M.; Peña, D. De; Merola, J. S. Extending the range of pentasubstituted cyclopentadienyl compounds : The synthesis of a series of tetramethyl (alkyl or aryl) cyclopentadienes (Cp / R), their iridium complexes and their catalytic activity for asymmetric transfer hydrogenation. *Polyhedron* **2014**, *84*, 120–135 DOI: 10.1016/j.poly.2014.06.053.
- (35) Liu, Z.; Habtemariam, A.; Pizarro, A. M.; Fletcher, S. A.; Kisova, A.; Vrana, O.; Salassa, L.; Bruijninx, P. C. A.; Clarkson, G. J.; Brabec, V.; et al. Organometallic Half-Sandwich Iridium Anticancer Complexes. **2011**, 3011–3026 DOI: 10.1021/jm2000932.
- (36) Gibson, C. P.; Bem, D. S.; Falloon, S. B.; Hitchens, T. K.; Cortopassi, J. E.; Virginia, W. Construction of Several Functionally-Substituted Tetramethylcyclopentadienyl Ligands , Their Use in the Syntheses of Several Organometallic Compounds , and Incorporation of the Organometallic Compounds into Polymers. **1992**, No. 5, 1742–1749 DOI: 10.1021/om00040a052.

This item was downloaded from IRIS Università di Bologna (<https://cris.unibo.it/>)

When citing, please refer to the published version.

- (37) Gorol, M.; Roesky, H. W.; Noltemeyer, M.; Schmidt, H.; Cyclopentadienyl, K.; P, O. (η^5 - Pentamethylcyclopentadienyl) iridium (III) Complexes with η^2 -N , O and η^2 -P , S Ligands. **2005**, 200500528, 4840–4844 DOI: 10.1002/ejic.200500528.
- (38) Bucci, A.; Savini, A.; Rocchigiani, L.; Zuccaccia, C.; Rizzato, S.; Albinati, A.; Llobet, A.; Macchioni, A. Organometallic iridium catalysts based on pyridinecarboxylate ligands for the oxidative splitting of water. *Organometallics* **2012**, 31 (23), 8071–8074 DOI: 10.1021/om301024s.
- (39) Hao, H.; Liu, X.; Ge, X.; Zhao, Y.; Tian, X.; Ren, T.; Wang, Y. Half-sandwich iridium (III) complexes with α -picolinic acid frameworks and antitumor applications. *J. Inorg. Biochem.* **2019**, 192 (October 2018), 52–61 DOI: 10.1016/j.jinorgbio.2018.12.012.
- (40) Blackmond, D. G. Reaction progress kinetic analysis: A powerful methodology for mechanistic studies of complex catalytic reactions. *Angew. Chemie - Int. Ed.* **2005**, 44 (28), 4302–4320 DOI: 10.1002/anie.200462544.
- (41) Blackmond, D. G. Kinetic Profiling of Catalytic Organic Reactions as a Mechanistic Tool. *J. Am. Chem. Soc.* **2015**, 137 (34), 10852–10866 DOI: 10.1021/jacs.5b05841.
- (42) Mills, A.; McMurray, N. Redox Catalysis. *J. Chem. Soc., Faraday Trans. 1* **1989**, 85 (8), 2047–2054.
- (43) Mills, A.; McMurray, N. Kinetic Study of the Oxidation of Water by CeIV Ions Mediated by Activated Ruthenium Dioxide Hydrate. *J. Chem. Soc., Faraday Trans. 1* **1989**, 85 (8), 2055–2070.
- (44) White, C.; Yates, A.; Maitlis, P. M.; Henekey, D. M. (η^5 -Pentamethylcyclopentadienyl)Rhodium and -Iridium Compounds. *Inorg. Synth.* **1992**, 29, 228–234.
- (45) Menges, F. Spectragryph - optical spectroscopy software, <http://www.effemm2.de/spectragryph>.

This item was downloaded from IRIS Università di Bologna (<https://cris.unibo.it/>)

When citing, please refer to the published version.

- (46) Fulmer, G. R.; Miller, A. J. M.; Sherden, N. H.; Gottlieb, H. E.; Nudelman, A.; Stoltz, B. M.; Bercaw, J. E.; Goldberg, K. I.; Gan, R.; Apiezon, H. NMR Chemical Shifts of Trace Impurities : Common Laboratory Solvents , Organics , and Gases in Deuterated Solvents Relevant to the Organometallic Chemist. *Organometallics* **2010**, *29*, 2176–2179 DOI: 10.1021/om100106e.
- (47) Willker, W.; Leibfritz, D.; Kerssebaum, R.; Bermel, W. Gradient Selection in Inverse Heteronuclear Correlation Spectroscopy. *Magn. Reson. Chem.* **1993**, *31*, 287–292.
- (48) Sheldrick, G. M. Crystal structure refinement with SHELXL. *Acta Cryst.* **2015**, *C71*, 3–8 DOI: 10.1107/S2053229614024218.
- (49) Gendve, U. De. On Enantiomorph-Polarity Estimation. *Acta Cryst.* **1983**, *A39*, 876–881.

BRIEFS (Word Style “BH_Briefs”). If you are submitting your paper to a journal that requires a brief, provide a one-sentence synopsis for inclusion in the Table of Contents.

SYNOPSIS (Word Style “SN_Synopsis_TOC”). If you are submitting your paper to a journal that requires a synopsis, see the journal’s Instructions for Authors for details.

This item was downloaded from IRIS Università di Bologna (<https://cris.unibo.it/>)

When citing, please refer to the published version.